

RESEARCH

Open Access



The role of endothelial cell-related gene COL1A1 in prostate cancer diagnosis and immunotherapy: insights from machine learning and single-cell analysis

Gujun Cong^{1†}, Jingjing Shao^{2†}, Feng Xiao^{3*}, Haixia Zhu^{2*} and Peipei Kang^{2*}

Abstract

Background Endothelial cells are integral components of the tumor microenvironment and play a multifaceted role in tumor immunotherapy. Targeting endothelial cells and related signaling pathways can improve the effectiveness of immunotherapy by normalizing tumor blood vessels and promoting immune cell infiltration. However, to date, there have been no comprehensive studies analyzing the role of endothelial cells in the diagnosis and treatment of prostate adenocarcinoma (PRAD).

Method By integrating clinical and transcriptomic data from TCGA-PRAD, we initially identified key endothelial cell-related genes in PRAD samples through single-cell analysis. Subsequently, cluster analysis was employed to classify PRAD samples based on the expression of these endothelial cell-related genes, allowing us to explore their correlation with patient prognosis and immunotherapy outcomes. A diagnostic model was then constructed and validated using a combination of 108 machine learning algorithms. The XGBoost and Random Forest algorithms highlighted the significant role of COL1A1, and we further analyzed the expression and correlation of COL1A1, AR, and EGFR through multiplex immunofluorescence staining. In vitro experimental analysis of the impact of COL1A1 on the progression of PRAD.

Results Single-cell analysis identified 12 differential prognostic genes associated with endothelial cells. Cluster analysis confirmed a strong correlation between endothelial cell-related genes and both prostate cancer prognosis and immunotherapy responses. Diagnostic models developed using various machine learning techniques demonstrated the significant predictive capability of these 12 genes in the diagnosis of prostate cancer. Furthermore, based on patients' prognostic information, multiple machine learning analyses highlighted the critical role of COL1A1.

[†]Gujun Cong and Jingjing Shao contributed equally to this work.

*Correspondence:

Feng Xiao
xfeng_1981@163.com
Haixia Zhu
00zlingling@163.com
Peipei Kang
15851269958@163.com

Full list of author information is available at the end of the article



Immunofluorescence analysis results confirmed that COL1A1 is highly expressed in prostate cancer and is positively correlated with both AR and EGFR. In vitro experiments confirm that reducing COL1A1 expression levels can inhibit PRAD progression.

Conclusion This study provides a comprehensive analysis of the role of endothelial cell-related genes in the diagnosis, prognosis, and immunotherapy of prostate cancer. The findings, supported by various machine learning algorithms and experimental results, highlight COL1A1 as a significant target for the diagnosis and immunotherapy of PRAD.

Keywords Single cell analysis, Machine learning, PRAD, Endothelial cell, COL1A1

Introduction

Prostate cancer is a type of malignant growth that begins in the prostate's epithelial cells, with prostate adenocarcinoma (PRAD) being the most common form of this disease [1, 2]. In the United States, projections indicate there will be 299,010 new cases diagnosed and 35,250 deaths attributable to the disease in 2024 [3]. The clinical progression of individuals with PRAD shows considerable variability; patients with localized PRAD often experience long survival durations without tumor advancement, whereas those with invasive or metastatic PRAD tend to experience swift progression and presently have limited treatment options available [4]. The management of PRAD heavily relies on androgen deprivation therapy (ADT). Nevertheless, within five years, approximately 10–20% of patients might advance to castration-resistant prostate cancer, and 15–33% may face the development of tumor metastasis [5]. These challenges significantly impact patient outcomes, underscoring the urgent necessity for enhanced treatment and monitoring methodologies.

The combination of single-cell analysis with machine learning in diagnosing and treating prostate cancer represents significant advancements in oncology, particularly in customizing patient care and improving treatment outcomes [6]. Single-cell analysis enables the exploration of individual cancer cells, providing crucial insights into their unique characteristics and responses to therapy, which is vital given the diversity observed within tumors [7, 8]. In conclusion, employing single-cell analysis and machine learning for prostate cancer diagnosis and therapy is reshaping the sphere of oncology. These advanced tools are essential for comprehending tumor diversity, anticipating treatment responses, and personalizing patient care, thus offering significant potential for better management of prostate cancer.

Recent research has highlighted the importance of endothelial cells in the development and spread of PRAD, along with their potential role as diagnostic biomarkers and therapeutic targets. An important observation reveals that endothelial cells originating from prostate tumors possess distinct angiogenic properties and express various receptors, including those for androgens

and VEGF. This indicates that such cells are actively involved in the tumor microenvironment, rather than simply acting as passive elements, thereby playing a crucial role in tumor growth and metastasis. For example, studies have shown that anti-angiogenic agents like Sunitinib and Sorafenib can impact the proliferation, survival, and movement of these endothelial cells associated with tumors, underscoring their promise as therapeutic targets in managing PRAD [9]. Furthermore, the regulation of particular genes within endothelial cells may act as indicators for PRAD. For instance, research on circulating tumor-associated endothelial cells has surfaced as a noteworthy method to enhance diagnostic precision for clinically important prostate cancer. Identifying tCECs in the bloodstream correlates with the presence of aggressive tumors, and analyzing these cells can significantly boost the positive predictive value (PPV) of prostate-specific antigen (PSA) testing, which often experiences low PPV [10]. This innovative approach could help in stratifying patients who require biopsy, thereby reducing unnecessary procedures and associated complications. In addition to their diagnostic potential, endothelial cells are also implicated in the therapeutic landscape of PRAD. The interaction between endothelial cells and prostate cancer cells can promote tumor invasion and metastasis through various signaling pathways. For instance, endothelial cells have been shown to secrete CCL5, which induces autophagy in prostate cancer cells, thereby enhancing their invasive capabilities. Targeting this CCL5/CCR5 signaling pathway, along with autophagy inhibition, has been proposed as a strategy to reduce metastasis in advanced prostate cancer models [11]. In our study, we conducted a comprehensive analysis of the role of endothelial cell-related genes in the diagnosis, prognosis, and immunotherapy of prostate cancer using single-cell analysis and machine learning algorithms. The XGBoost and Random Forest algorithms consistently identified COL1A1 as one of the top five genes associated with the prognosis of patients with prostate cancer (PRAD). Utilizing the GOsemsim algorithm, we elucidated the significant role of COL1A1 as an endothelial cell-related gene. The insights gained from studying these cells may lead to the development of improved diagnostic

tools and novel treatment strategies, ultimately enhancing the management of this prevalent malignancy.

Materials and methods

Datasets and patient samples

The TCGA database comprises data from 52 normal prostate samples alongside 498 samples of PRAD. The diagnostic model related to endothelial cell genes was assessed using the GSE14206 (53 tumor samples and 14 normal prostate samples), GSE46602 (36 tumor samples and 14 normal prostate samples), GSE6956 (69 tumor samples and 20 normal prostate samples), and GSE71016 (48 tumor samples and 47 normal prostate samples) datasets. Furthermore, 100 prostate cancer tissue cases and 50 adjacent non-cancerous tissue cases were sourced from Shanghai Outdo Biotech Company.

Cluster analysis

Expression profiles derived from RNA sequencing and pertinent clinical data for PRAD were sourced from the TCGA database. Consistency analysis was conducted using the ConsensusClusterPlus R package (v1.54.0), which permitted a maximum of six clusters while sampling 80% of the total samples across 100 iterations. The 'hc' clustering algorithm was utilized, integrating the inner linkage method 'ward.D2'. Heatmaps for clustering were generated employing the pheatmap package in R (v1.0.12) [12].

Analysis of the correlation between endothelial cell-related gene and immune cell infiltration

To guarantee an accurate evaluation of immune scores, we made use of immunedeconv, an R package that incorporates six of the latest algorithms designed to assess immune cell infiltration: TIMER, xCell, MCP-counter, CIBERSORT, EPIC, and quanTIseq [13, 14]. Each of these algorithms has been thoroughly benchmarked, showcasing its distinct performance and benefits. In our research, we focused particularly on the MCP-counter algorithm for our analysis. In addition, the GSE141445 data set in the TISCH2 database is also used to perform immune analysis from the perspective of single cell analysis [15].

Constructing diagnostic model

In order to create a highly accurate and consistently performing diagnosis model for PRAD, we incorporate a variety of machine learning algorithms in different configurations. The training dataset includes data from TCGA-PRAD, while validation is carried out with the GSE14206, GSE46602, GSE6956, and GSE71016 datasets.

Immunofluorescence method to analyze the expression of COL1A1, AR and EGFR in PRAD tissue

The sections were subsequently placed into a repair box containing a pH 9.0 EDTA alkaline antigen repair solution and subjected to heating in a pressure cooker for 2 min. After allowing them to cool under natural conditions, the sections were washed three times with PBS (pH 7.4), each wash lasting 5 min with gentle shaking. Following this, they were incubated for a duration of 15 min in a 3% hydrogen peroxide solution, maintained at room temperature and shielded from light. A blocking solution was then applied dropwise to ensure complete coverage of the tissue, followed by a blocking period of 30 min at room temperature. Afterward, antibodies targeting COL1A1 (67288-1-Ig), AR (22089-1-AP), and EGFR (18986-1-AP) were diluted in an antibody diluent and added to each section, which were then incubated overnight at 4 °C. The following day, the sections underwent three additional washes with PBS, with each wash lasting 5 min. Once excess liquid was gently shaken off, a poly-HRP secondary antibody that matched the primary antibody's species was applied dropwise and incubated at room temperature in the dark for 10 to 20 min.

Gene enrichment analysis

The Limma package from R software (version 3.40.2) was employed to assess the differential expression of COL1A1 mRNA. In order to further explore the functions of potential targets, we performed a functional enrichment analysis on the resulting data. The KEGG enrichment analysis acts as a useful resource for examining gene functions and related high-level genomic functional details. To enhance our comprehension of the oncogenic functions of the target genes, we utilized the ClusterProfiler package in R to analyze the Gene Ontology (GO) functionalities of the potential mRNAs and enrich the KEGG pathways [16].

Cell culture and transient transfection

The DU145 and PC3 cell lines were obtained from the Shanghai Institutes of Biological Sciences. Primary human umbilical vein endothelial cells were purchased from Shanghai Zhongqiao Xinzhou Biotechnology Co., Ltd. The DU145 cells were cultured in RPMI 1640 medium, supplemented with 10% fetal bovine serum, 100 U/mL penicillin, and 100 µg/mL streptomycin. PC3 cells were cultured in F-12K medium, which contained equal concentrations of penicillin, streptomycin, and FBS as those used for the DU145 cells. All cell lines were incubated in a 37°C environment with 5% CO₂. All siRNAs used in this study (siCOL1A1#1: 5'-CGGCCAACCCUGG UGCUAAATT-3', siCOL1A1#2: 5'-GAAAUCAACCCG AGGAAUUTT-3') were purchased from general biological company.

Quantitative real-time polymerase chain reaction (qRT-PCR)

Total RNA was extracted from DU145 cell line using TRIzol reagent. For cDNA synthesis, 500 ng of RNA was utilized with the HiScript II SuperMix. The SYBR Green Master Mix facilitated the qRT-PCR process in the ABI 7500 System. The conditions for PCR amplification included 45 cycles consisting of 10 min at 94 °C, followed by 10 s at 94 °C, and then 45 s at 60 °C. GAPDH served as the internal reference. Below is the list of primer pair sequences for the target genes: VEGFC (Forward: GCG CTGATCCCCAGTCCG, Reverse: AGGACAGACATCA GCTCATC), VEGFR1 (Forward: GGCCCGGGATATTT ATAAGAAC, Reverse: CCATCCATTTTAGGGGAAGT C) and GAPDH (Forward: CGGAGTCAACGGATTTG GTCGTAT, Reverse: AGCCTTCTCCATGGTGGTGAA GAC).

Transwell migration and invasion assays

Migration experiments commence by placing Transwell inserts into a 24-well plate. An appropriate volume of 250 µL of serum-free medium is added to the upper chamber of each Transwell, while 700 µL of serum-containing medium is introduced into the lower chamber. Cultured cells are washed with sterile PBS, followed by digestion with trypsin, which is subsequently halted by adding the cell mixture to a tube containing serum-free medium. The cells are then counted, and the cell suspension is adjusted to the desired concentration before adding 200 µL of the cell suspension to the upper chamber of the Transwell. Care should be taken to avoid the formation of bubbles. The Transwell plate is incubated at 37 °C with 5% CO₂ for 24–48 h to facilitate cell migration. Upon completion of the incubation period, the Transwell insert is removed. The upper chamber is gently washed with sterile PBS to eliminate non-migrated cells, and the migrated cells in the lower chamber are fixed using a fixative. After fixation, a PBS wash is performed, followed by staining with 0.1% crystal violet. For the invasion experiment, a layer of Matrigel is evenly coated in the upper chamber of the Transwell, in accordance with the aforementioned protocol.

Cell scratch and proliferation assays

Cell scratching experiment: First, culture cells in an appropriate dish until they reach approximately 80–90% confluence. Use a sterile pipette tip or scratching tool to create a scratch in the cell monolayer, simulating a wound. Gently wash the dish to remove floating cells, then add fresh culture medium. Immediately observe the cells using a microscope and capture images at the 0-hour mark. Place the Petri dish back into the incubator. After 24 h, remove the culture dish, observe the cells again, and take additional images to assess cell migration.

The proliferation experiment consists of CCK8 and colony formation assays. For the CCK8 assay, first prepare a 96-well cell culture plate and add 1,000 treated cells per well. Once the cells have adhered, add 10 µL of CCK8 reagent to each well. The results obtained after a 2-hour incubation period are considered the 0-hour results. Samples are then incubated under the same conditions for specified durations (24, 48, or 72 h) before detection. For colony formation assays, treated cells were plated at a density of 3,000 cells per well. After a duration of 5 days, the cells were fixed using a fixative and subsequently stained with crystal violet.

Flow cytometry

Collect the cells from each group in the control group and the siCOL1A1 group for flow cytometry analysis. Digest the cells with 0.25% trypsin at room temperature for 10 min, then centrifuge at 1200 rpm for 15 min. Collect the cell pellet and wash it three times with PBS. Prepare a cell suspension at a concentration of 1×10^5 cells/ml. Take 100 µL of this 1×10^5 cell suspension and add a fluorescently labeled phenotypic antibody CD31 (14-0319-82). Incubate, wash, and then analyze using the flow cytometer to assess surface antigen expression in each group.

Western-blot

Total protein was extracted from cells or tissues utilizing RIPA buffer. Following quantification, equal quantities of protein were separated using 10% SDS-PAGE and subsequently transferred to a PVDF membrane. The membrane was blocked with 5% skim milk for 2 h, and the antibodies were incubated overnight at 4 °C. After this, a secondary antibody was applied to the membrane and incubated at room temperature for 2 h. The visualization of immunoblotting was achieved with an ECL kit and analyzed using Chemiluminescent Imaging.

Statistical analysis

The expression levels of genes associated with endothelial cells in both PRAD and normal tissues were evaluated using the Wilcoxon rank-sum test. Prognostic analysis was conducted using the log-rank test. Spearman correlation analysis was employed to assess correlations between quantitative variables that do not follow a normal distribution. A significance level of less than 0.05 was set to determine statistical relevance.

Result

The level of endothelial cell infiltration is related to the prognosis of PRAD patients

In the TCGA-PRAD dataset, we examined the variations in the infiltration levels of different immune cell types in PRAD samples as opposed to normal prostate samples

by utilizing the MCP-counter algorithm. Our examination uncovered notable disparities in the infiltration levels of endothelial cells, neutrophils, myeloid dendritic cells, macrophages/monocytes, monocytes, NK cells, and T lymphocytes (Fig. 1A-B). The abundance percentage of immune cells infiltrating tumors for each sample was then depicted as a heat map (Fig. 1C). Furthermore, the Kaplan-Meier (KM) curve demonstrated the relationship between various immune cell types and patient

prognosis. It was particularly noteworthy that the levels of B cell and endothelial cell infiltration were significantly linked to patient outcomes; in particular, increased levels of these two immune cell types were associated with worse prognoses (Fig. 1D). Since no significant difference was observed in B cell infiltration levels between PRAD and normal prostate samples, our future research will mainly concentrate on endothelial cells.

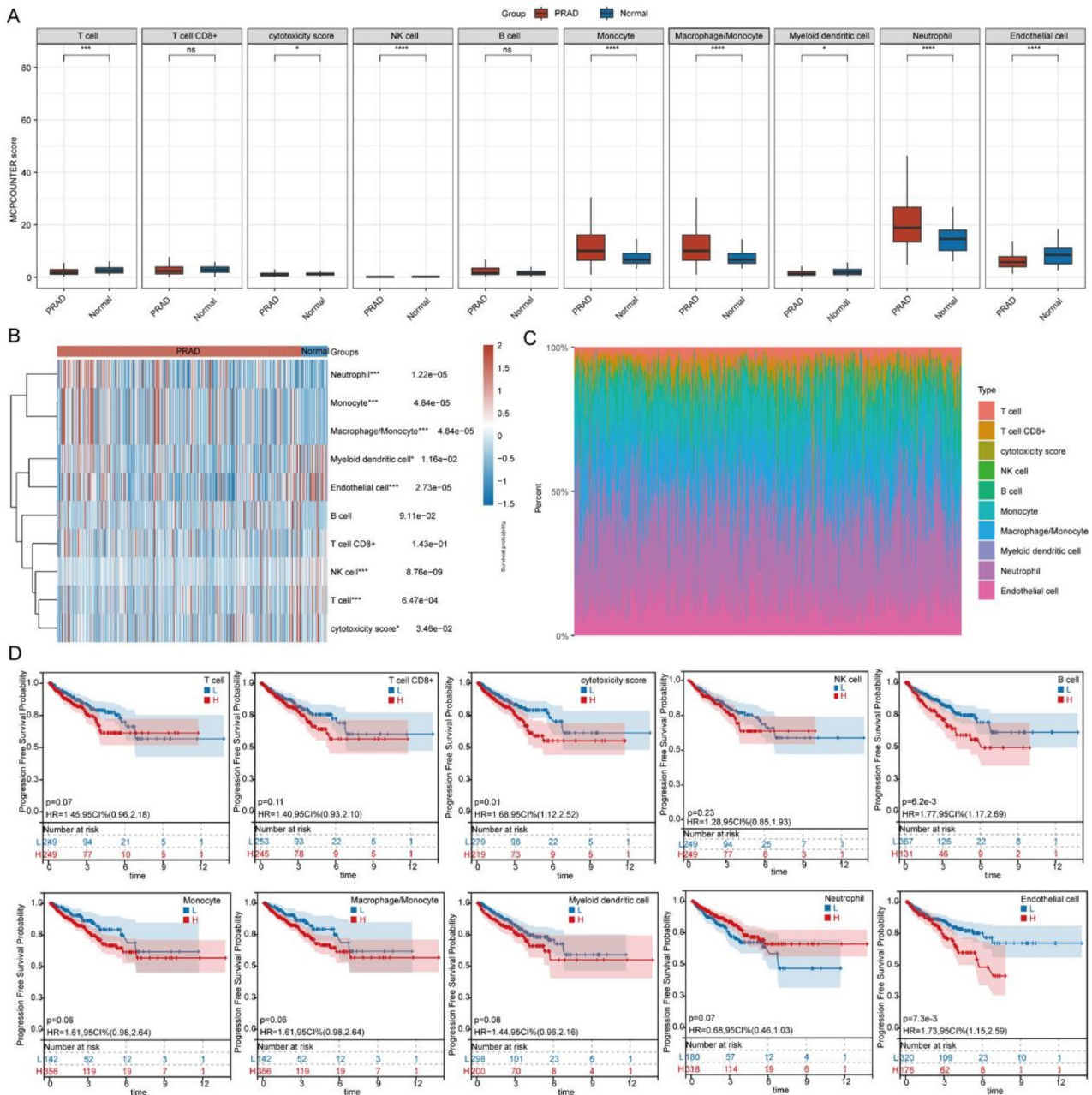


Fig. 1 Levels of infiltration by high endothelial cells correlate with unfavorable outcomes for patients. (A-B) Variations in the infiltration levels of various immune cell types in PRAD compared to normal prostate tissue samples. (C) The proportional representation of tumor-infiltrating immune cells across the samples. (D) The prognostic significance of distinct immune cell populations in PRAD

Identifying key endothelial cell genes

Single-cell RNA sequencing (scRNA-seq) is a powerful technique for investigating the heterogeneity of cell type composition within the tumor microenvironment (TME). TISCH2 is a dedicated scRNA-seq database that focuses on TME-related datasets. Utilizing the TISCH2 database, we analyzed the infiltration differences of various immune cells within the GSE141445 dataset. Employing single-cell analysis technology, the samples in the GSE141445 dataset were categorized into eight distinct cell groups (Fig. 2A-B). The predominant cell type identified was epithelial cells, followed by endothelial cells (Fig. 2C-D). We then collected genes exhibiting a Log2 fold change (Log2FC) greater than 1 and a p-value less than 0.5, which were subsequently screened against clinical information from the TCGA-PRAD dataset. Ultimately, we identified 12 differential prognostic genes related to endothelial cells. Violin plots illustrate the expression levels of these 12 genes across different immune cell types (Fig. 2E-F). Finally, the expression and prognostic differences of these 12 endothelial cell-related genes are presented through box plots and forest plots (Fig. 2G-H).

Cluster analysis

In recent years, the concept of precision medicine has advanced the study of subgroup typing among individual research subjects. In our study, we further investigated the functions of endothelial cell-related genes through cluster analysis. Based on the cumulative distribution function (CDF) curve and the CDF delta area curve, we opted to divide the TCGA-PRAD samples into two clusters. Furthermore, we deduced the ideal number of clusters by identifying the K value that corresponds to the lowest Proportion of Ambiguous Clusters (PAC) score. PAC measures the intermediate section, which is defined as the percentage of sample pairs where the consensus index lies within the range $(u_1, u_2) \in [0, 1]$. In this context, u_1 approaches 0, and u_2 approaches 1 (for instance, $u_1=0.1$ and $u_2=0.9$). A decrease in PAC values denotes a more level middle area and a lesser frequency of inconsistent classifications in the permuted clustering experiments. In conclusion, we recognized $K=2$ as the best grouping option (Fig. 3A-D). We also analyzed the expression differences of 12 endothelial cell-related genes between cluster 1 and cluster 2, presenting the results through heat maps and box plots (Fig. 3E-G). Subsequently, we examined the differences in progression-free survival (PFS) and disease-free survival (DFS) among patients in the two clusters, revealing that patient in cluster 2 experienced worse PFS and DFS (Fig. 3H-I). Given the significant role of gene mutations in tumor progression, we also analyzed the top ten genes with high mutation rates in the two clusters (Fig. 3J-K). Finally, we

explored the potential mechanisms underlying the prognostic differences between patients in cluster 1 and cluster 2 using KEGG analysis. Our findings indicated that the cAMP signaling pathway was significantly enriched in cluster 1, while the PI3K-AKT signaling pathway and multiple immune-related pathways were enriched in cluster 2 (Fig. 3L-M).

Endothelial cell-related genes associated with immunotherapy in PRAD patients

The growth and development of tumors are closely associated with immune cells in their microenvironment [17, 18]. Analyzing immune infiltration can enhance our understanding of how various types of immune cells influence tumor initiation, progression, and metastasis. In our analysis, we observed significant differences in the presence of endothelial cells, myeloid dendritic cells, macrophages/monocytes, monocytes, B cells, NK cells, CD8+T cells, and T cells overall (Fig. 4A). Subsequently, we examined the expression differences of immune checkpoint-related genes across the two clusters, identifying significant variations in *ITPRIPL1*, *SIGLEC15*, *TIGIT*, *PDCD1LG2*, *PDCD1*, *LAG3*, *HAVCR2*, *CTLA4*, and *CD274* (Fig. 4B). We further illustrated the expression differences of immune checkpoint genes in distinct clusters using heat maps (Fig. 4C). Immune checkpoint blockade (ICB) therapy has transformed the treatment landscape for human cancers, and we employed the Tumor Immune Dysfunction and Exclusion (TIDE) algorithm to predict the response of different clusters to potential immune checkpoint inhibitors. Our findings indicated that cluster 2 exhibited significantly higher TIDE scores compared to cluster 1 (Fig. 4D). TIDE employs a set of gene expression markers to assess two different mechanisms by which tumors evade the immune response: the impairment of tumor-infiltrating cytotoxic T lymphocytes (CTLs) and the rejection of CTLs due to immunosuppressive elements. An elevated TIDE score is associated with lower effectiveness of ICB therapy and a decreased survival duration following ICB treatment. As a result, individuals classified in cluster 2 are expected to have less favorable ICB results, indicating a grim prognosis tied to this cluster. Finally, we examined the distribution of patients across various clinical stages within the separate clusters. Our results reveal significant differences in the population distribution of clusters 1 and 2 concerning T stage, N stage, and various tumor outcomes (Fig. 4E-H).

Build a diagnostic model

To enable the prompt identification of patients with PRAD, our objective was to create a diagnostic model focused on this condition. The initial training phase made use of the TCGA-PRAD dataset, while subsequent

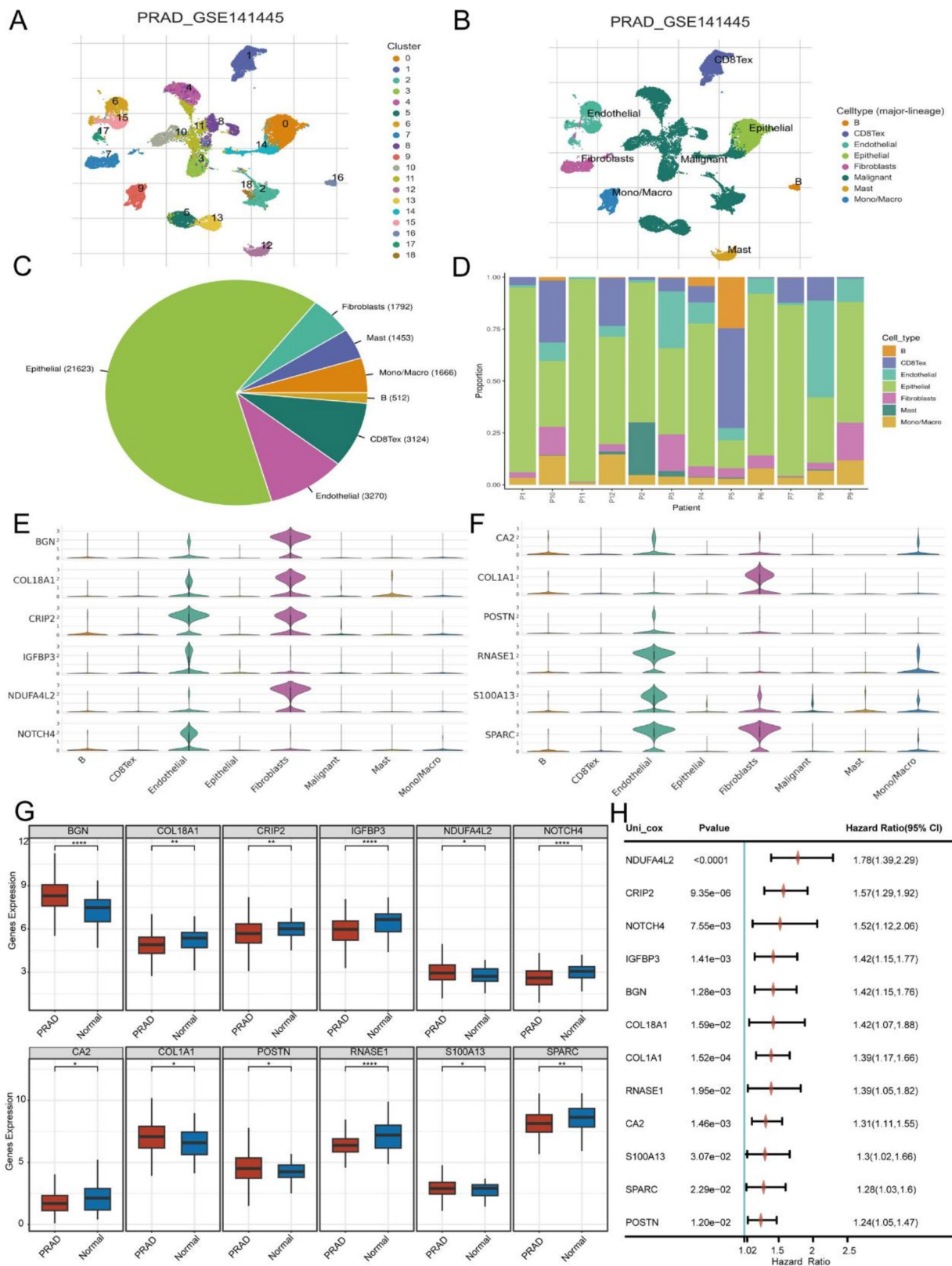


Fig. 2 Identified 12 key regulatory genes of endothelial cells. **(A-D)** Identification of regulatory genes in endothelial cells utilizing a single-cell analysis technique. **(E-F)** Variation in the expression of 12 genes regulated by endothelial cells across various immune cell types. **(G)** Differential expression analysis of 12 endothelial cell-regulated genes within the TCGA-PRAD dataset. **(H)** Prognostic variations linked to 12 endothelial cell regulatory genes in the TCGA-PRAD dataset

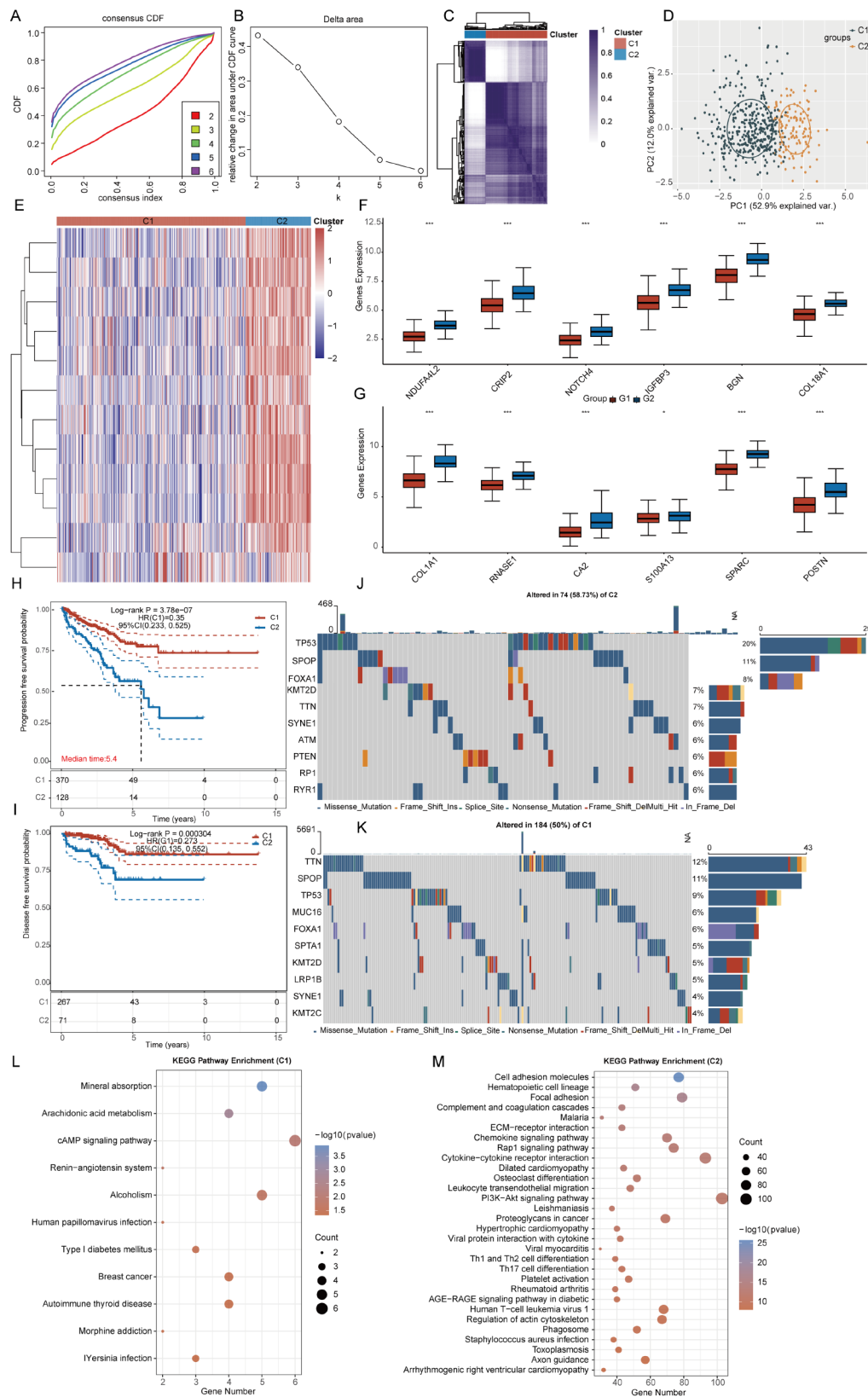


Fig. 3 Subgroup classification. **(A)** Cumulative Distribution Function curve. **(B)** CDF Delta area curve. **(C)** The heat map of the consensus clustering. **(D)** Consensus clustering group diagram. **(E-G)** Expression analysis of endothelial cell-related genes. **(H-I)** Prognostic analysis among different clusters. **(J-K)** Mutation analysis of different clusters. **(L-M)** Gene enrichment analysis of different clusters

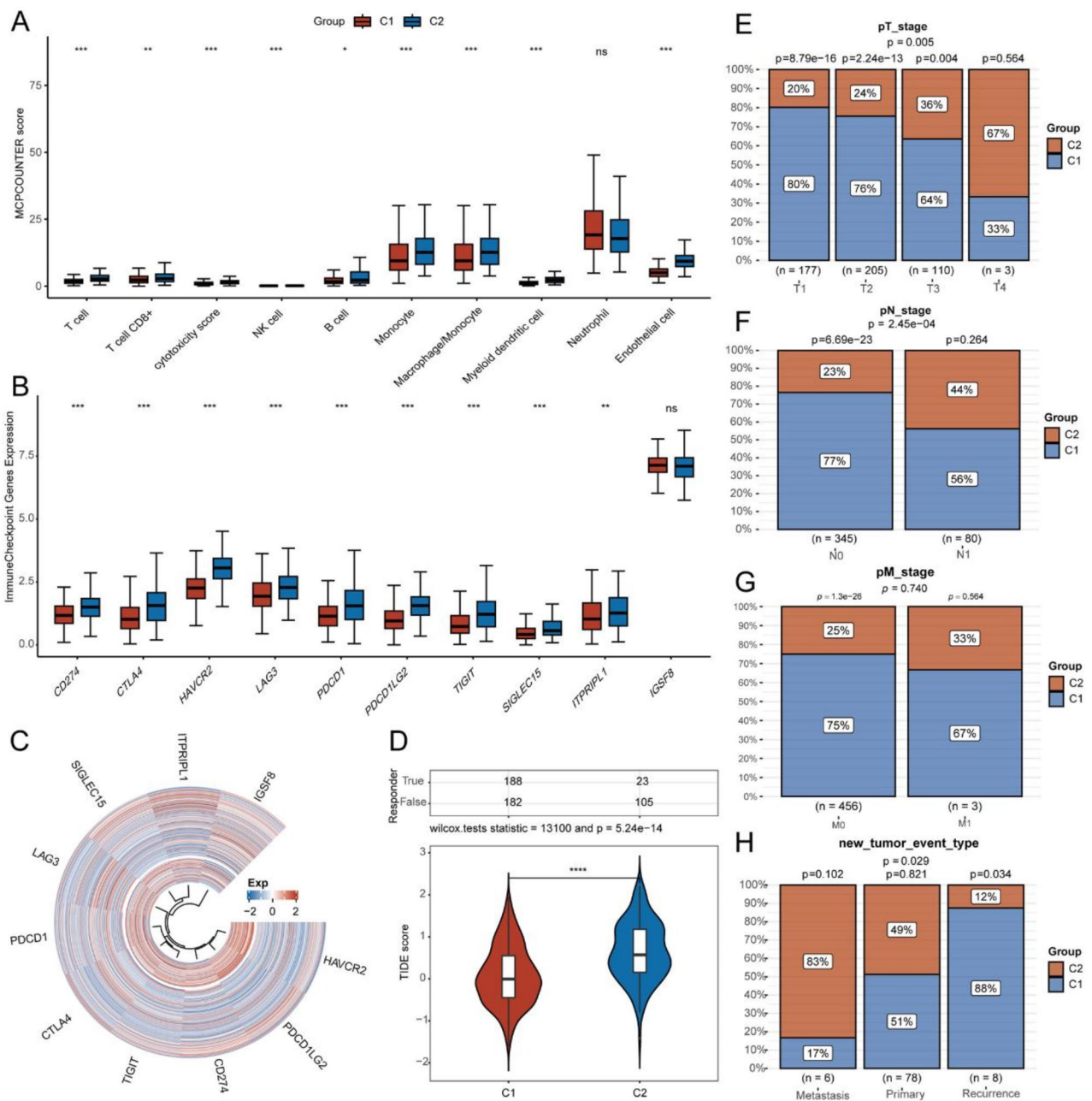


Fig. 4 Endothelial cell-related genes linked to immunotherapy efficacy. **(A)** Analysis of immune cell infiltration levels in different clusters. **(B-C)** Expression analysis of immune checkpoint-related genes in different clusters. **(D)** Analysis of the effects of ICB treatment on different clusters of patients. **(E-H)** Population distribution of patients in different clusters in different clinical stages

validation incorporated four other datasets: GSE14206, GSE46602, GSE6956, and GSE71016. We first illustrated the predictive potential of 12 genes associated with endothelial cells for the onset of PRAD, analyzing this across the five datasets with the help of ROC curves (Fig. 5A). Following this, we combined different machine learning techniques to advance the development of predictive models for diagnosing PRAD. Among several machine learning combinations, the plsRglm algorithm pair was

identified as the most successful in terms of constructing models (Fig. 5B). The AUC for the TCGA-PRAD training dataset reached 0.917, while the AUC values for the validation datasets GSE14206, GSE46602, GSE6956, and GSE71016 were 0.693, 0.742, 0.808, and 0.715, respectively. This model employed the 12 endothelial cell-related genes through the plsRglm algorithm (Fig. 5C).

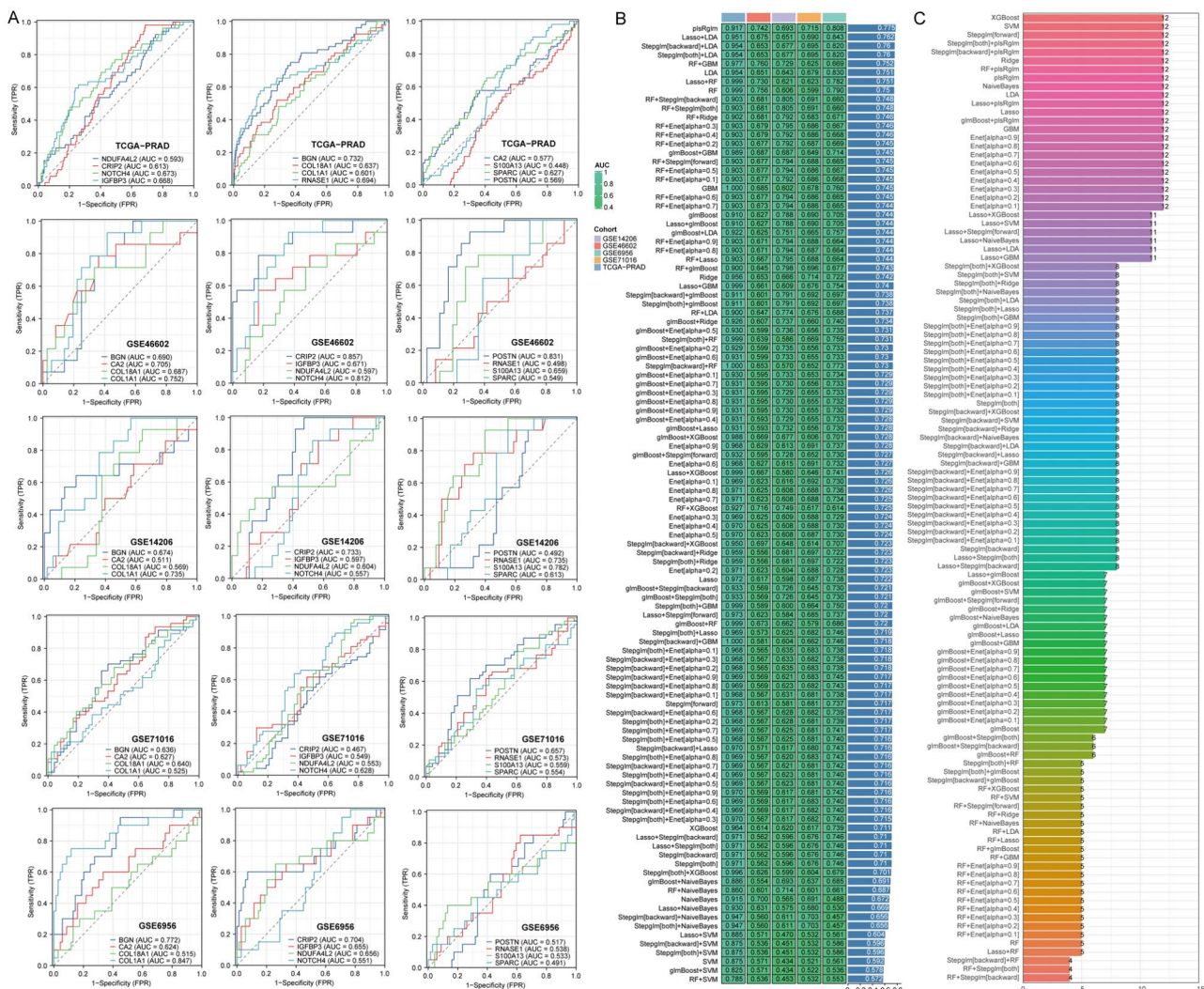


Fig. 5 Optimal diagnostic models identified through machine learning algorithms. **(A)** Diagnostic relevance of genes in models across multiple datasets. **(B)** AUC value comparison among diagnostic models developed using different combinations of algorithms. **(C)** Count of genes included in diagnostic models constructed with various algorithm pairings

Machine learning analysis identifies key endothelial cell regulatory genes

Based on the MCP-counter algorithm, we determined the endothelial cell infiltration level for each sample in the TCGA-PRAD dataset. We analyzed and compared the correlation between 12 endothelial cell-related genes and the endothelial cell infiltration score. Our results indicated that, with the exception of S100A13, there was no significant correlation between the remaining genes and the level of endothelial cell infiltration; however, the other 11 endothelial cell-related genes were all positively correlated with the endothelial cell infiltration score (Fig. 6A). Subsequently, we employed the XGBoost algorithm and the random forest algorithm to rank the importance of the endothelial cell-related genes by grouping the outcomes of patients’ PFS. Additionally, we utilized the GOsemsim algorithm to rank the genes

based on their similarity (Fig. 6B-D). Our analysis results highlight the critical role of COL1A1, which was found to be positively correlated with the infiltration levels of various immune cells (Fig. 6E). Furthermore, patients exhibiting high expression levels of COL1A1 demonstrated a poor response to immune checkpoint blockade (ICB) treatment (Fig. 6F). Finally, we stratified the TCGA-PRAD dataset according to COL1A1 expression and analyzed the distribution of patients across different clinical stages (Fig. 6G-K).

Functional analysis of COL1A1

In the TCGA-PRAD dataset, we initially classified the samples according to the median expression levels of COL1A1, dividing them into groups of high and low COL1A1 expression, followed by a differential analysis (Fig. 7A-B). The results of the KEGG analysis indicated

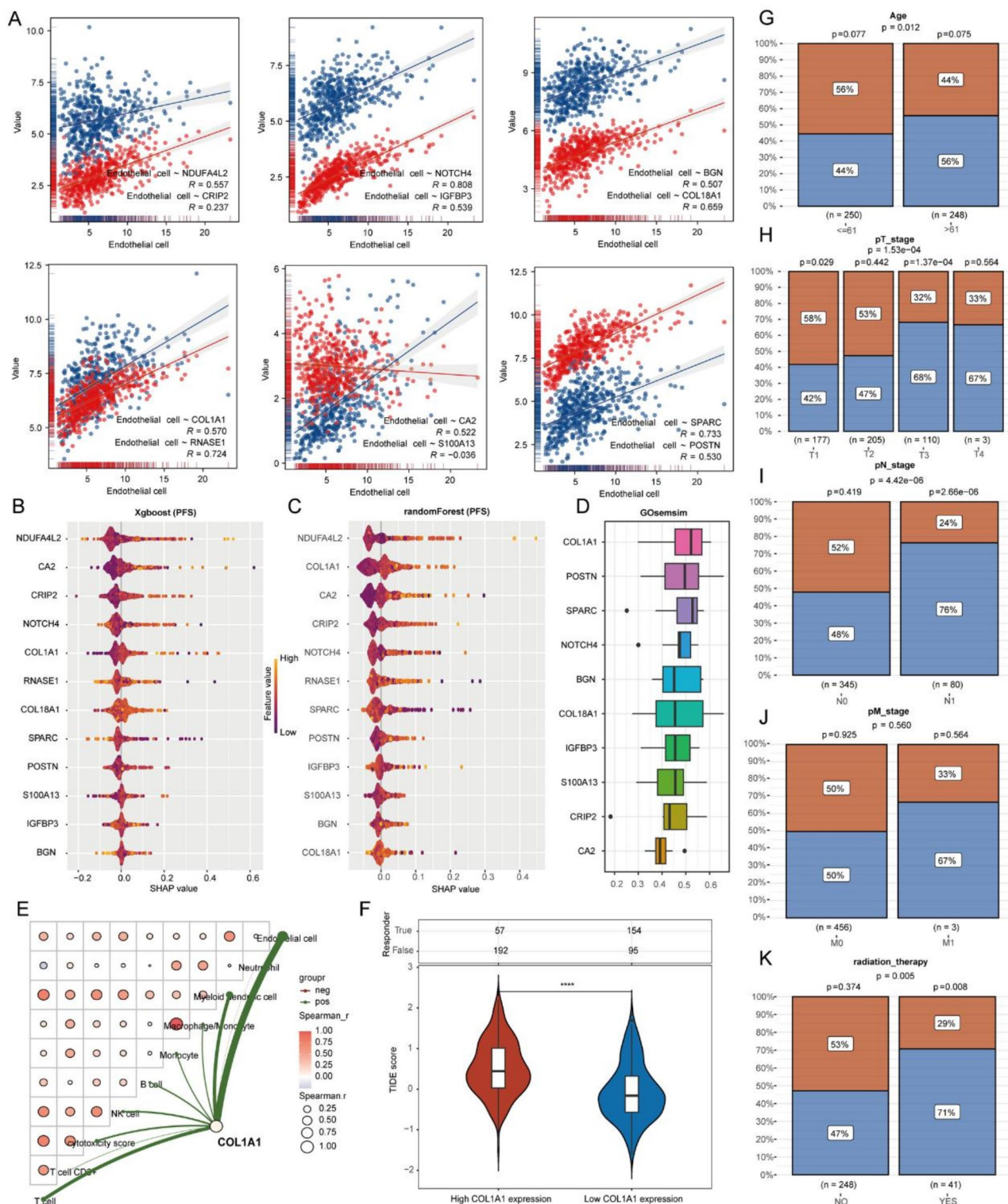


Fig. 6 COL1A1 is identified as a key regulatory gene of endothelial cells. **(A)** Correlation analysis between endothelial cell-related genes and endothelial cell infiltration scores. **(B)** XGBoost algorithm identifies key genes related to PFS in PRAD. **(C)** Random forest algorithm identifies key genes related to PFS in PRAD. **(D)** G0semsim algorithm ranks genes by importance. **(E)** Analysis of the correlation between COL1A1 and immune infiltration. **(F)** Analysis of the correlation between COL1A1 and immunotherapy. **(G-K)** Correlation analysis between COL1A1 expression and different clinical stages

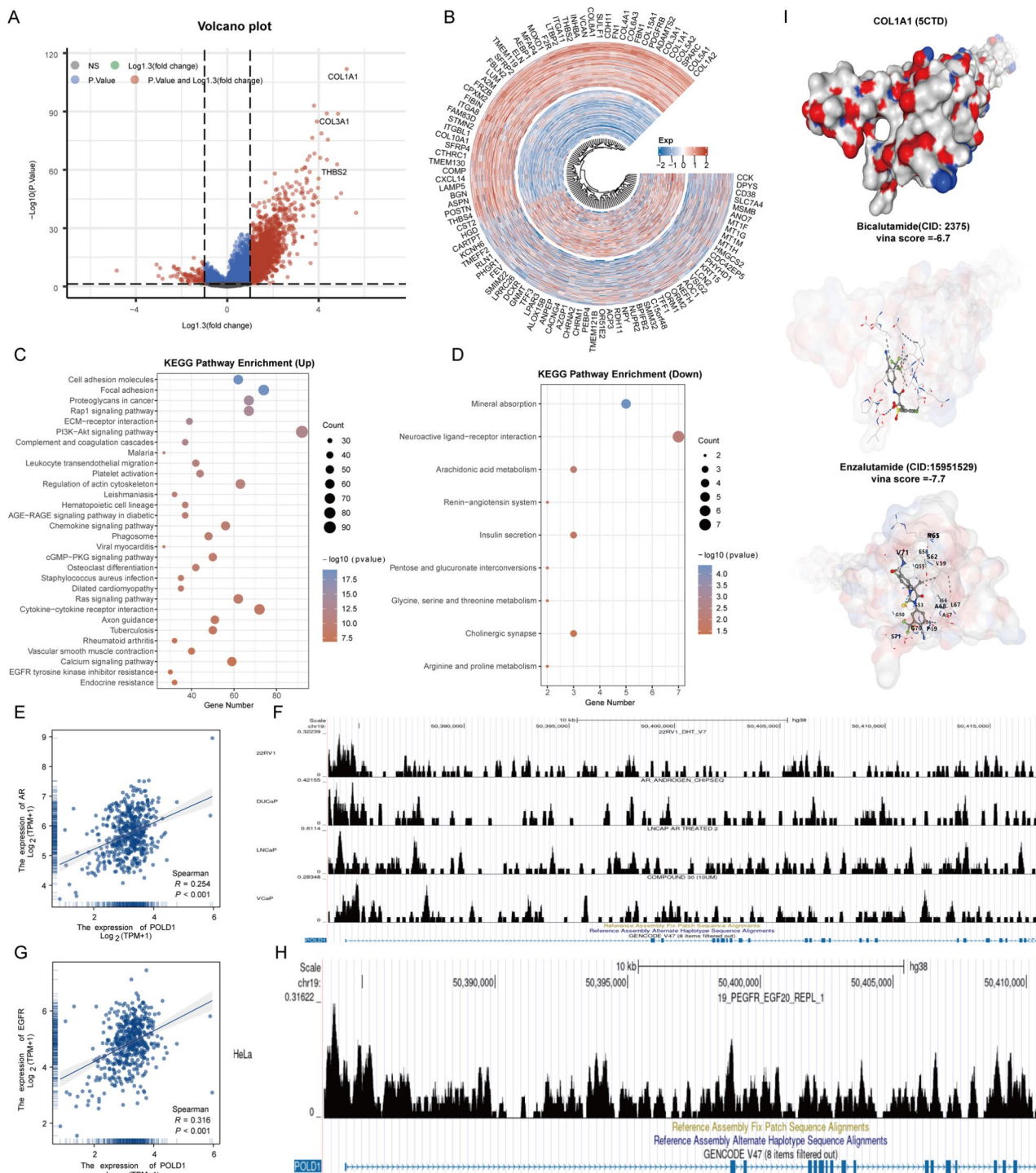


Fig. 7 COL1A1 is positively related to AR and EGFR. **(A)** Difference analysis volcano plot. **(B)** Difference analysis heat map. **(C-D)** KEGG analysis. **(E-F)** Correlation analysis between COL1A1 and AR. **(G-H)** Correlation analysis between COL1A1 and EGFR. **(I)** Molecular docking of COL1A1 and PRAD therapeutic drugs

that among the upregulated genes, pathways such as the PI3K–Akt signaling pathway, cytokine–cytokine receptor interaction, EGFR tyrosine kinase inhibitor resistance, and endocrine resistance were significantly

enriched (Fig. 7C). Conversely, among the downregulated genes, pathways like neuroactive ligand–receptor interaction were identified as enriched (Fig. 7D). Based on these findings, we established a notable relationship

between COL1A1 and resistance to endocrine therapy as well as EGFR tyrosine kinase inhibitors. Therefore, we proceeded to analyze the correlation between COL1A1 and androgen receptor (AR) and EGFR. Our results demonstrated that COL1A1 was positively correlated with both AR and EGFR. Since AR and EGFR are recognized as transcription factors, we investigated if COL1A1 is influenced at the transcriptional level by AR and EGFR, which was confirmed by our findings (Fig. 7E-H). Additionally, we explored the connection between COL1A1 and AR-targeting medications via molecular docking analysis. The results from the docking study suggested that COL1A1 exhibits a significant binding affinity for both bicalutamide and enzalutamide (Fig. 7I).

Multiple immunofluorescence staining analysis of the correlation between COL1A1, AR and EGFR

To delve deeper into the relationship between COL1A1, AR, and EGFR, we carried out an extensive analysis utilizing a PRAD tissue chip. Our study involved the examination of 100 PRAD tissue samples, beginning with the assessment of the link between COL1A1 and AR. We presented immunofluorescence images showing COL1A1 and AR for two of the samples, as well as images displaying COL1A1 and EGFR for another pair of samples (Fig. 8A-B). A scatter plot demonstrated the relationship between COL1A1 and AR, indicating a positive correlation with a coefficient of 0.351 (Fig. 8C). In a similar fashion, COL1A1 showed a positive correlation with EGFR, achieving a coefficient of 0.328 (Fig. 8D). Lastly, we examined the relationship between EGFR and AR, confirming that AR also exhibits a positive correlation with EGFR (Fig. 8E).

Expression analysis of COL1A1

In this part, we individually illustrate the expression variation of the critical gene COL1A1 in PRAD in relation to genes associated with endothelial cells (Fig. 9A). The box plot demonstrates a notable increase in COL1A1 expression in PRAD when compared to normal tissues (Fig. 9B). Additionally, we examined COL1A1 expression across various T stages and N stages, showing that COL1A1 levels are greater in both advanced T stages and heightened N stages (Fig. 9C-D).

Knockdown of COL1A1 inhibits PRAD progression

Initially, we downregulated the expression of COL1A1 in the PRAD cell lines DU145 and PC3. Our findings indicated that siCOL1A1#1 was more effective in inhibiting COL1A1 expression in both DU145 and PC3 (Fig. 10A). We conducted CCK8 and colony formation assays to assess the changes in the proliferation capacity of PRAD cells following COL1A1 knockdown. Our experiments demonstrated that silencing COL1A1

significantly reduced the proliferation of DU145 and PC3 cell lines (Fig. 10B-E). Given the established relationship between endothelial cells and angiogenesis, we also investigated the impact of COL1A1 knockdown on angiogenic processes. The results revealed that silencing COL1A1 markedly inhibited the angiogenic potential of PRAD (Fig. 10F). Furthermore, we examined the effect of COL1A1 knockdown on the metastatic capabilities of DU145 and PC3. Our data confirmed that the metastatic potential of both DU145 and PC3 was significantly diminished following the introduction of siCOL1A1#1 (Fig. 10G-J). CD31 has been identified as a marker for PRAD endothelial cells, while VEGFC and VEGFR1 have been shown to play crucial regulatory roles concerning PRAD endothelial cells. Correlation analysis indicated a positive association between COL1A1 and CD31, VEGFC, and VEGFR1 (Fig. 10K). Additionally, in DU145 cells, we analyzed the effects of siCOL1A1#1 on the expression levels of VEGFC and VEGFR1 mRNA. We found that knocking down COL1A1 inhibited the expression levels of VEGFC and VEGFR1 (Fig. 10L). Additionally, we analyzed the impact of COL1A1 knockdown on the number of CD31-positive cells, revealing a significant reduction in their quantity following COL1A1 knockdown (Fig. 10M). Collectively, these findings confirm that the knockdown of COL1A1 inhibits PRAD progression by regulating endothelial cell dynamics.

Discussion

The treatment of patients with PRAD has advanced significantly over the past few decades, with options including surgery, radiation therapy, chemotherapy, and hormonal therapy [19]. However, the effectiveness of these treatments remains limited. Notably, 5% of PRAD cases are metastatic at initial diagnosis, and the five-year survival rate is less than 30%. This highlights the urgent need for the development of new therapeutic targets [20]. Identifying novel targets could facilitate the discovery of biomarkers for PRAD, thereby enhancing early screening and diagnosis. Early detection is crucial for improving disease outcomes and increasing cure rates [21]. Furthermore, by pinpointing new treatment targets, personalized treatment plans can be devised. This allows for the selection of corresponding targeted therapies or immunotherapies tailored to the patient's specific genetic background and tumor characteristics, ultimately reducing unnecessary side effects and improving treatment efficacy.

Endothelial cells are vital in the advancement and spread of PRAD, affecting various elements of tumor biology, such as angiogenesis, adhesion of cells, and the characteristics of the tumor microenvironment. The relationship between PRAD cells and endothelial cells is intricate, encompassing numerous signaling pathways and mechanisms. A key role of endothelial cells in the

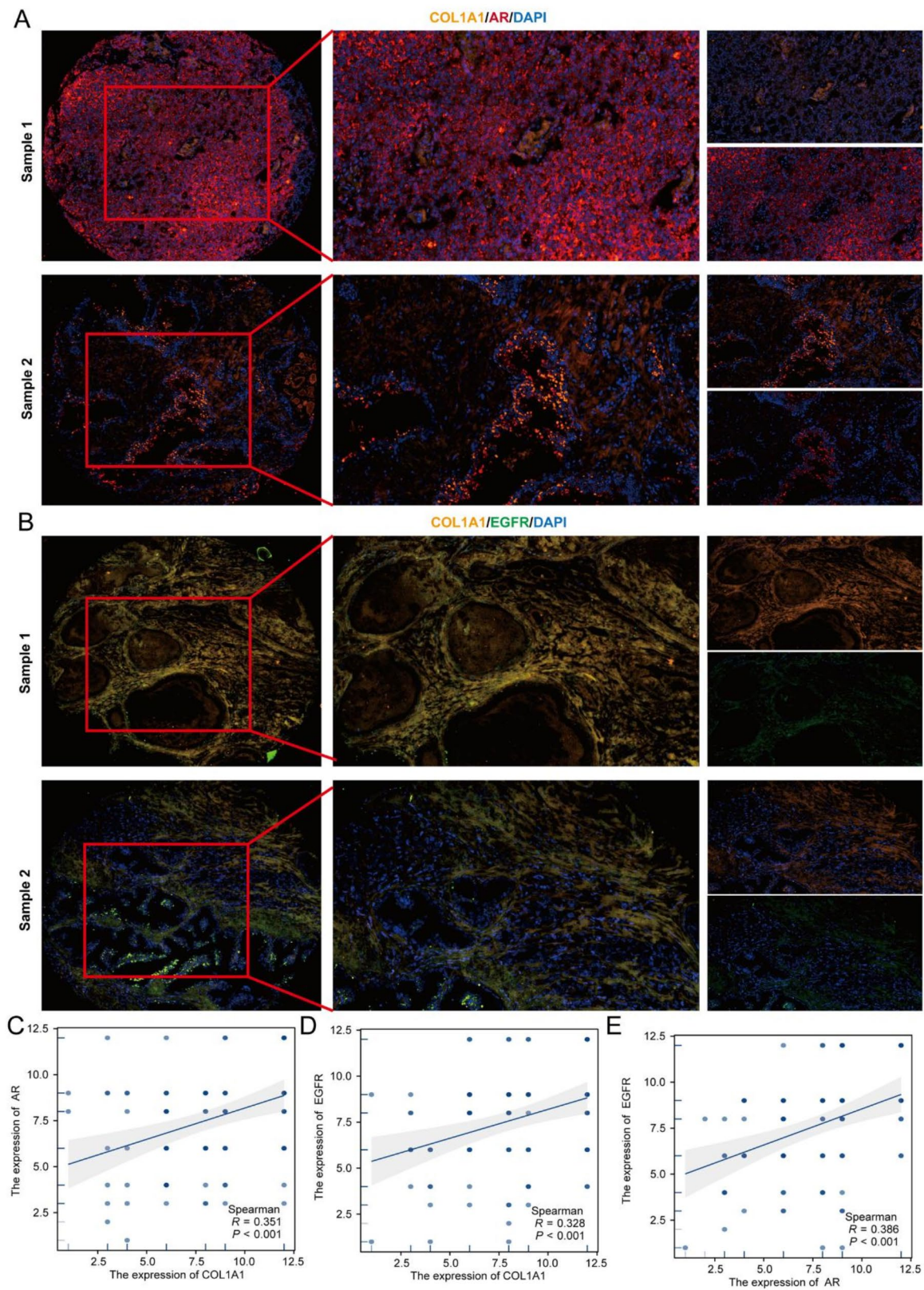


Fig. 8 COL1A1 is positively correlated with both AR and EGFR. **(A)** Expression of COL1A1 and AR. **(B)** Expression of COL1A1 and EGFR. **(C)** Scatter plot of correlation between COL1A1 and AR. **(D)** Scatter plot of correlation between COL1A1 and EGFR. **(E)** Scatter plot of correlation between EGFR and AR

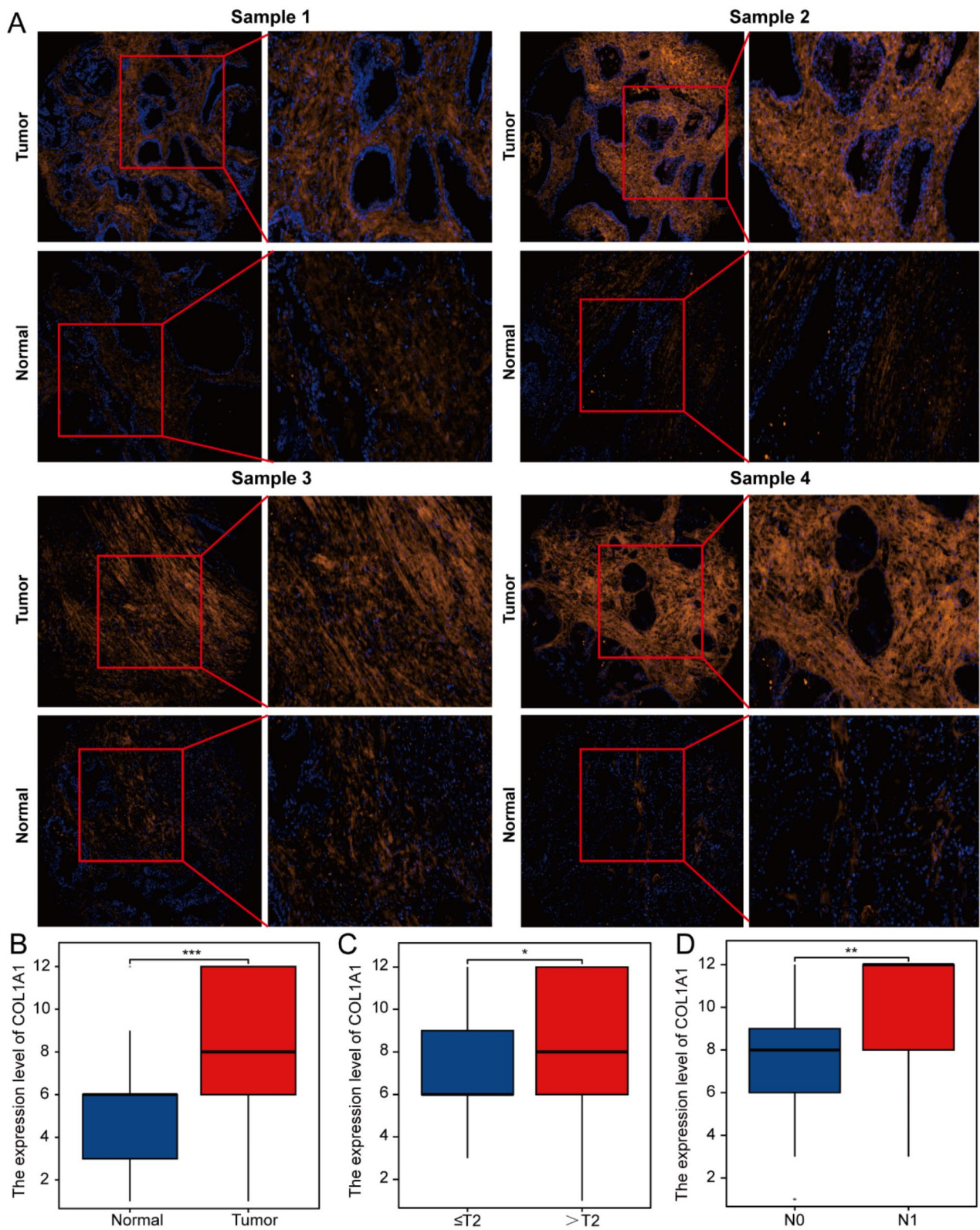


Fig. 9 COL1A1 is highly expressed in PRAD. **(A-B)** Expression analysis of COL1A1 in PRAD. **(C)** Expression analysis of COL1A1 in different T stages of PRAD. **(D)** Expression analysis of COL1A1 in different N stages of PRAD

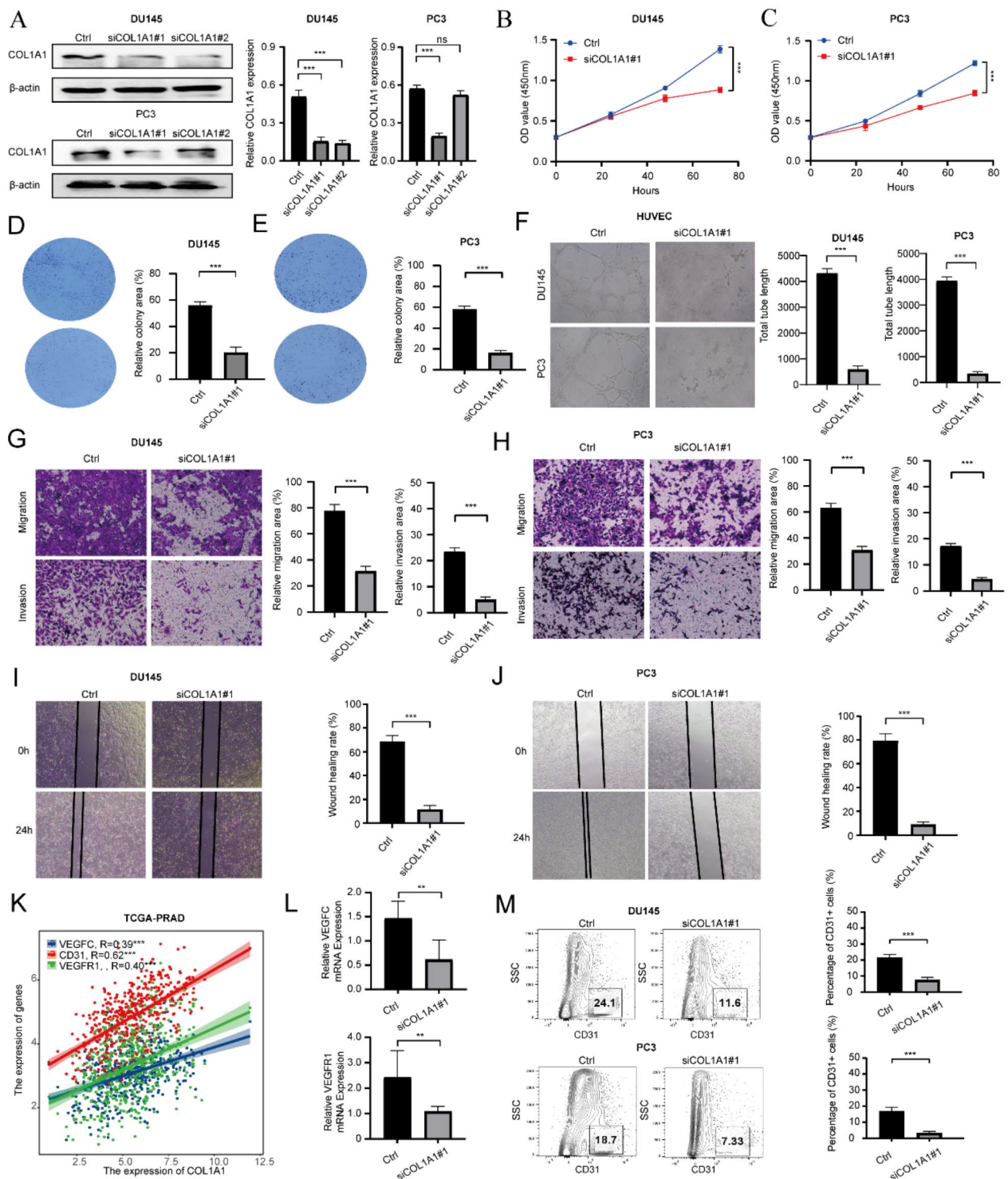


Fig. 10 Knockdown of COL1A1 regulates PRAD endothelial cells. **(A)** Validation of knockdown of COL1A1 in PRAD cells. **(B-C)** CCK8 analyzes the effect of COL1A1 on tumor proliferation ability. **(D-E)** Clonogenic assay to analyze the effect of COL1A1 on tumor proliferation. **(F)** Effects of knocking down COL1A1 on tumor angiogenesis. **(G-H)** Effects of knocking down COL1A1 on tumor migration and invasion ability. **(I-J)** Effects of knocking down COL1A1 on tumor metastasis ability. **(K)** Correlation analysis between COL1A1 and endothelial cell markers. **(L)** Effects of knocking down COL1A1 on the expression of endothelial cell markers. **(M)** Effects of knocking down COL1A1 on the number of CD31-positive cells

context of PRAD is their participation in angiogenesis, which is the formation of new blood vessels from existing ones. This mechanism is critical for both tumor growth and metastasis since tumors depend on a blood supply for essential nutrients and oxygen. In our study, we found that the prognosis of PRAD patients was worse when the level of endothelial cell infiltration increased, which also reflects the oncogenicity of endothelial cells in PRAD. Through single-cell analysis, we identified 12 differential prognostic genes associated with endothelial cells. Notably, *NDUFA4L2* has been linked to endothelial cells in both liver and renal cancers [22, 23]. Furthermore, inhibiting *Notch4* expression has been shown to reduce tumor growth in mouse cancer models by targeting tumor endothelial cells [24]. *SPARC* also plays a crucial role in maintaining endothelial barrier function. Research indicates that *SPARC* expression is upregulated in response to pro-inflammatory stimuli, which correlates with increased paracellular permeability and decreased transendothelial electrical resistance in endothelial cells. These findings suggest that *SPARC* may influence the integrity of the endothelial barrier during inflammatory responses [25]. Additionally, *IGFBP3* has been demonstrated to reduce the adhesion of human umbilical vein endothelial cells to the extracellular matrix by downregulating the transcription of integrins. This inhibition of integrin expression results in decreased phosphorylation of FAK and Src, which are critical components of the signaling pathways that mediate cell adhesion and migration. The disruption of these pathways indicates that *IGFBP3* can effectively interfere with adhesion signaling in endothelial cells, potentially impacting processes such as angiogenesis and tumor metastasis [26]. Lastly, studies have shown that *BGN* promotes the expression of VEGF through its interaction with Toll-like receptors on endothelial cells, thereby activating downstream signaling pathways and enhancing endothelial cell function [27]. However, no studies have yet confirmed the relationship between *COL18A1*, *CRIP2*, *S100A13*, and other genes in relation to their regulatory interactions with endothelial cells.

Subsequently, through multiple machine learning methods, we analyzed the role of endothelial cell-related genes in PRAD immunotherapy. In the context of immunotherapy, targeting the interactions between endothelial cells and PRAD cells presents a potential strategy to enhance treatment efficacy. Additionally, the modulation of endothelial cell function may enhance the infiltration and activity of immune cells within the tumor, potentially reversing the immunosuppressive effects of the TME. Furthermore, the role of endothelial cells in angiogenesis is critical in PRAD. The formation of new blood vessels not only supports tumor growth but also influences the distribution and efficacy of immune cells within the TME. By targeting endothelial cell functions,

such as angiogenesis, researchers aim to improve the delivery and effectiveness of immunotherapeutic agents [28]. Overall, the interplay between endothelial cells and PRAD cells is complex and multifaceted. Understanding these interactions is crucial for developing more effective immunotherapy strategies. By targeting the mechanisms through which endothelial cells influence tumor progression and immune evasion, it may be possible to enhance the efficacy of existing immunotherapies and develop novel treatment approaches for PRAD.

Based on the XGBoost and random forest algorithms, we found that *COL1A1*, an endothelial cell-related gene, exhibited a strong correlation with patient PFS. Furthermore, utilizing the GOsemsim algorithm, we conclude that *COL1A1* is the most significant gene among the endothelial cell-related genes included in our analysis. Recent studies have highlighted the complex interactions between *COL1A1* expression and various immune components, which can influence the efficacy of immunotherapeutic strategies. Specifically, *COL1A1* expression has been positively correlated with the abundance of cancer-associated fibroblasts (CAFs) and macrophage infiltration in several cancers, including gastrointestinal cancers, bladder cancer, and head and neck squamous cell carcinoma [29]. This relationship indicates that *COL1A1* might be involved in influencing the immunosuppressive TME, typically marked by the existence of immune cells that can hinder effective anti-tumor reactions. Moreover, the expression of *COL1A1* has been found to be negatively correlated with the quantity of CD8+T cells in certain cancers, indicating that higher levels of *COL1A1* may be associated with reduced infiltration of cytotoxic T cells, which are crucial for effective anti-tumor immunity [30]. This relationship underscores the potential of *COL1A1* as a marker for immunoresistance, where tumors evade immune detection and destruction. In conclusion, *COL1A1* plays a pivotal role in tumor immunotherapy by influencing the TME and immune cell dynamics. However, the role of *COL1A1* in PRAD has not yet been documented. In our study, we identified *COL1A1* as a potential target for immunotherapy in patients with PRAD. Furthermore, through gene enrichment analysis, we discovered that *COL1A1* is strongly associated with AR and EGFR. Consequently, we analyzed the correlation among these three genes using immunofluorescence staining, and our findings were validated at the protein level. Finally, through cell experiments, we demonstrated the potential of *COL1A1* as a therapeutic target for PRAD. The expression level of *COL1A1* can serve as a biomarker to assess the response of prostate cancer patients to various treatment options. By quantifying *COL1A1* expression, clinicians can more accurately predict patient prognosis and develop personalized treatment plans. Furthermore, considering the role

of COL1A1 in the tumor microenvironment, the development of targeted therapies against COL1A1 may offer new treatment alternatives for prostate cancer patients. Such targeted therapies could be combined with existing hormone therapies or immunotherapies to enhance efficacy and mitigate drug resistance.

Conclusion

Through the application of single-cell analysis technology and machine learning, we identified the critical role of endothelial cell-related genes in PRAD. COL1A1, recognized as an endothelial cell-related gene, may serve as a potential immunotherapy target for patients with PRAD.

Author contributions

Gujun Cong and Jingjing Shao drafted the manuscript, Haixia Zhu conducted preliminary investigations. Peipei Kang and Feng Xiao were responsible for reviewing it. All authors have read and approved the final manuscript.

Funding

This study was supported by Nantong Health Commission (ONZ2023055 and MS2023063), Scientific research project of Nantong Health Commission (MS2022041) and Nantong University Clinical Medicine Special Research fund (2023JY014).

Data availability

No datasets were generated or analysed during the current study.

Declarations

Ethics approval and consent to participate

This study was approved by the Ethics Committee of Shanghai Outdo Biotech Company. All patients provided written informed consent prior to enrollment in the study.

Competing interests

The authors assert that the study was carried out with no commercial or financial affiliations that could be interpreted as a possible conflict of interest.

Author details

- ¹Clinical Laboratory Center, Affiliated Mental Health Center of Nantong University (Nantong Fourth People's Hospital, Nantong, China
- ²Cancer Research Center Nantong, Affiliated Tumor Hospital of Nantong University & Nantong Tumor Hospital, Nantong, China
- ³Department of Pathology, Affiliated Nantong Hospital 3 of Nantong University (Nantong Third People's Hospital), Nantong, China

Received: 5 December 2024 / Accepted: 28 December 2024

Published online: 08 January 2025

References

1. Wang Y, Li C, He J, Zhao Q, Zhou Y, Sun H, Zhu H, Ding B, Ren M. Multi-omics analysis and experimental validation of the value of monocyte-associated features in prostate cancer prognosis and immunotherapy. *Front Immunol.* 2024;01-01; 15 1426474. <https://doi.org/10.3389/fimmu.2024.1426474>. PMID: 38947325.
2. Wang Y, He J, Zhao Q, Bo J, Zhou Y, Sun H, Ding B, Ren M. Evaluating the predictive value of angiogenesis-related genes for prognosis and immunotherapy response in prostate adenocarcinoma using machine learning and experimental approaches. *Front Immunol.* 2024;01-01; 15 1416914. <https://doi.org/10.3389/fimmu.2024.1416914>. PMID: 38817605.
3. Siegel RL, Giaquinto AN, Jemal A, Cancer statistics, *Cancer JC.* 2024 Jan-Feb;74(1):12–49. doi: 10.3322/caac.21820. Epub 2024 Jan 17. Erratum in: CA

- Cancer J Clin. 2024 Mar-Apr;74(2):203. <https://doi.org/10.3322/caac.21830>. PMID: 38230766.
4. Sartor O. Localized Prostate Cancer - Then and Now. *N, Engl. J Med.* 2023;388(17):1617–1618. doi: 10.1056/NEJMe2300807. Epub 2023 Mar 11. PMID: 36912567.
5. Wang Y, Ji B, Zhang L, Wang J, He J, Ding B, Ren M. Identification of metastasis-related genes for predicting prostate cancer diagnosis, metastasis and immunotherapy drug candidates using machine learning approaches. *Biol Direct.* 2024;06-25; 19 (1): 50. <https://doi.org/10.1186/s13062-024-00494-x>. PMID: 38918844.
6. Wang Y, Ma L, He J, Gu H, Zhu H. Identification of cancer stem cell-related genes through single cells and machine learning for predicting prostate cancer prognosis and immunotherapy. *Front Immunol.* 2024;01-01; 15 1464698. <https://doi.org/10.3389/fimmu.2024.1464698>. PMID: 39267762.
7. Zulibiyah A, Wen J, Yu H, Chen X, Xu L, Ma X, Zhang B. Single-cell RNA sequencing reveals potential for endothelial-to-mesenchymal transition in tetralogy of fallot. *Congenit Heart Dis.* 2023;18(6):611–25. <https://doi.org/10.32604/chd.2023.047689>.
8. XU Y, CHENG D, L HU, DONG, X, LV L, ZHANG C, ZHOU. J. single-cell sequencing analysis reveals the molecular mechanism of promotion of SCAP proliferation upon AZD2858 treatment *BIOCELL.* 2023-01-01; 47 (4): 825–36. <https://doi.org/10.32604/biocell.2023.026122>
9. Fiorio Pla A, Brossa A, Bernardini M, Genova T, Grolez G, Villers A, Leroy X, Prevarskaya N, Gkika D, Bussolati B. Differential sensitivity of prostate tumor derived endothelial cells to sorafenib and sunitinib. *BMC Cancer.* 2014;14:939. <https://doi.org/10.1186/1471-2407-14-939>. PMID: 25494980.
10. Bhakdi SC, Suriyaphol P, Thaicharoen P, Grote STK, Komoltri C, Chaiyaprasithi B, Charnkaew K. Accuracy of Tumour-Associated circulating endothelial cells as a screening biomarker for clinically significant prostate Cancer cancers (Basel). 2019;11 (8):null. <https://doi.org/10.3390/cancers11081064>. PMID: 31357651.
11. Zhao R, Bei XYB, Wang X, Jiang C, Shi F, Wang X, Zhu Y, Jing Y, Han B, Xia S, Jiang Q. Endothelial cells promote metastasis of prostate cancer by enhancing autophagy. *J Exp Clin Cancer Res.* 2018;37(1):221. <https://doi.org/10.1186/s13046-018-0884-2>. PMID: 30200999.
12. Wang Y, Zhu H, Zhang L, He J, Bo J, Wang J, Ding B, Ren M. Common immunological and prognostic features of lung and bladder cancer via smoking-related genes: PRR11 gene as potential immunotherapeutic target. *J Cell Mol Med.* 2024;28(10):e18384. <https://doi.org/10.1111/jcmm.18384>. PMID: 38760964; PMCID: PMC11101993.
13. Newman AM, Liu CL, Green MR, Gentles AJ, Feng W, Xu Y, Hoang CD, Diehn M, Alizadeh AA. Robust enumeration of cell subsets from tissue expression profiles. *Nat Methods.* 2015;12(5):453–7. <https://doi.org/10.1038/nmeth.3337>. Epub 2015 Mar 30. PMID: 25822800; PMCID: PMC4739640.
14. Wang Y, Wang J, Zhang L, He J, Ji B, Wang J, Ding B, Ren M. Unveiling the role of YARS1 in bladder cancer: A prognostic biomarker and therapeutic target. *J CELL MOL MED.* 2024-04-01; 28 (7): 1–20. <https://doi.org/10.1111/jcmm.18213>. PMID: 38506098.
15. Han Y, Wang Y, Dong X, Sun D, Liu Z, Yue J, Wang H, Li T, Wang C. TISCH2: expanded datasets and new tools for single-cell transcriptome analyses of the tumor microenvironment. *Nucleic Acids Res.* 2023;51(D1):D1425–31. <https://doi.org/10.1093/nar/gkac959>. PMID: 36321662; PMCID: PMC9825603.
16. Wang JF, Wang JS, Liu Y, Ji B, Ding BC, Wang YX, Ren MH. Knockdown of integrin $\beta 1$ inhibits proliferation and promotes apoptosis in bladder cancer cells. *BIOFACTORS.* 2024-12-07; <https://doi.org/10.1002/biof.2150>. PMID: 39644117.
17. SHI J, ZHANG Y, CHEN, Y, GUO T, PIAO H. Identification of TMEM159 as a biomarker of glioblastoma progression based on immune characteristics *BIOCELL.* 2024-01-01; 0 (0): 1–10. <https://doi.org/10.32604/biocell.2024.051049>
18. ZHAI X, LIU J, XIAO J, ZHANG T, WANG J, LI J, YU S. The lactylation index predicts the immune microenvironment and prognosis of pan-cancer patients. *BIOCELL.* 2024-01-01; 0 (0): 1–10. <https://doi.org/10.32604/biocell.2024.050803>.
19. Kang Z, Wan ZH, Gao RC, Chen DN, Zheng QS, Xue XY, Xu N, Wei Y. Disulfidoptosis-related subtype and prognostic signature in prostate cancer. *Biol Direct.* 2024;19(1):97. <https://doi.org/10.1186/s13062-024-00544-4>. PMID: 39444006; PMCID: PMC11515740.
20. Kadeerhan G, Xue B, Wu XL, Chen WN, Wang DW. Incidence trends and survival of metastatic prostate cancer with bone and visceral involvement: 2010–2019 surveillance, epidemiology, and end results. *Front Oncol.* 2023;13:1201753. <https://doi.org/10.3389/fonc.2023.1201753>. PMID: 37601697; PMCID: PMC10435983.
21. Sabater A, Sanchis P, Seniuk R, Pascual G, Anselmino N, Alonso DF, Cayol F, Vazquez E, Marti M, Cotignola J, Toro A, Labanca E, Bizzotto J, Gueron G.

- Unmasking Neuroendocrine Prostate Cancer with a Machine Learning-Driven Seven-Gene Stemness Signature That Predicts Progression. *Int J Mol Sci.* 2024-10-22; 25 (21): <https://doi.org/10.3390/ijms252111356>. PMID: 39518911.
22. Zheng Q, Lu C, Yu L, Zhan Y, Chen Z. Exploring the metastasis-related biomarker and carcinogenic mechanism in liver cancer based on single cell technology. *Heliyon.* 2024-03-30; 10 (6): e27473. <https://doi.org/10.1016/j.heliyon.2024.e27473>. PMID: 38509894.
 23. Su C, Lv Y, Lu W, Yu Z, Ye Y, Guo B, Liu D, Yan H, Li T, Zhang Q, Cheng J, Mo Z. Single-Cell RNA Sequencing in Multiple Pathologic Types of Renal Cell Carcinoma Revealed Novel Potential Tumor-Specific Markers. *Front Oncol.* 2021-01-01; 11 719564. <https://doi.org/10.3389/fonc.2021.719564>. PMID: 34722263.
 24. Eng JW, Kato Y, Adachi Y, Swaminathan B, Naiche LA, Vadakath R, Sakamoto Y, Nakazawa Y, Tachino S, Ito K, Abe T, Minoshima Y, Hoshino-Negishi K, Ogasawara H, Kawakatsu T, Nishimura M, Katayama M, Shimizu M, Tahara K, Sato T, Suzuki K, Agarwala K, Iwata M, Nomoto K, Ozawa Y, Imai T, Funahashi Y, Matsui J, Kitajewski J. Inhibition of Notch4 using Novel neutralizing antibodies reduces Tumor Growth in Murine Cancer models by targeting the Tumor Endothelium. *Cancer Res Commun.* 2024;4(7):1881–93. <https://doi.org/10.1158/2767-9764.CRC-24-0081>. PMID: 38984877; PMCID: PMC11289863.
 25. Alkabi S, Basivireddy J, Zhou L, Roskams J, Rieckmann P, Quandt JA. SPARC expression by cerebral microvascular endothelial cells in vitro and its influence on blood-brain barrier properties. *J Neuroinflammation.* 2016;13(1):225. <https://doi.org/10.1186/s12974-016-0657-9>. PMID:27581191.
 26. Lee HJ, Lee JS, Hwang SJ, Lee HY. Insulin-like growth factor binding protein-3 inhibits cell adhesion via suppression of integrin β 4 expression *Oncotarget.* 2015;6 (17):15150–63. <https://doi.org/10.18632/oncotarget.3825>. PMID:25945837.
 27. Park ES, Kim S, Yao DC, Savarraj JP, Choi HA, Chen PRKE. Soluble Endoglin stimulates inflammatory and angiogenic responses in Microglia that Are Associated with endothelial dysfunction. *Int J Mol Sci.* 2022;23(3). <https://doi.org/10.3390/ijms23031225>. PMID:35163148.
 28. Qiao L, Liang Y, Li N, Lu Y, Zheng Q. Endothelin-A receptor antagonists in prostate cancer treatment-a meta-analysis *Int J Clin Exp Med.* 2015 undefined;8 (3):3465-73. doi: PMID:26064237.
 29. Liu Y, Xue JZM, Wang Z, Prognostic Prediction. Immune Microenvironment, and Drug Resistance Value of Collagen Type I Alpha 1 Chain: From Gastrointestinal Cancers to Pan-Cancer Analysis *Front Mol Biosci.* 2021 undefined;8:692120. <https://doi.org/10.3389/fmolb.2021.692120>. PMID:34395525.
 30. Zhu H, Hu X, Feng S, Jian Z, Xu X, Gu L, Xiong X. The Hypoxia-Related Gene COL5A1 Is a Prognostic and Immunological Biomarker for Multiple Human Tumors *Oxid Med Cell Longev.* 2022 undefined;2022:6419695. <https://doi.org/10.1155/2022/6419695>. PMID:35082969.

Publisher's note

Springer Nature remains neutral with regard to jurisdictional claims in published maps and institutional affiliations.